Supplementary Information

Probiotic intervention mitigates radiation-induced intestinal injury by alleviating oxidative stress in a human gut-on-a-chip

Nam Than[1], Tadanori Mammoto[2,6], Donald E. Ingber[2,3,4,*], and Hyun Jung Kim[1,5*]

[1]Department of Inflammation and Immunity, Cleveland Clinic, Cleveland, OH 44195, USA
[2]Wyss Institute for Biologically Inspired Engineering at Harvard University, Boston, MA 02115, USA
[3]Harvard Medical School & Vascular Biology Program, Boston Children's Hospital, Boston, MA 02115, USA
[4]Harvard School of Engineering and Applied Sciences, Harvard University, Cambridge, MA 02138, USA
[5]Cleveland Clinic Lerner College of Medicine of Case Western Reserve University, Cleveland, OH 44195, USA
[6]Current address: Department of Pediatrics, Medical College of Wisconsin, Milwaukee, WI 53226, USA

***Correspondence to:**

Hyun Jung Kim, PhD
Department of Inflammation and Immunity
Cleveland Clinic
9500 Euclid Ave., NE3
Cleveland, OH 44195, USA
Phone: 216-445-8148
Email: kim19@ccf.org

Or

Donald E. Ingber, MD, PhD
Wyss Institute for Biologically Inspired Engineering at Harvard University
201 Brookline Ave., Suite 401,
Boston, MA 02115.
Phone: 617-432-7044
Email: don.ingber@wyss.harvard.edu

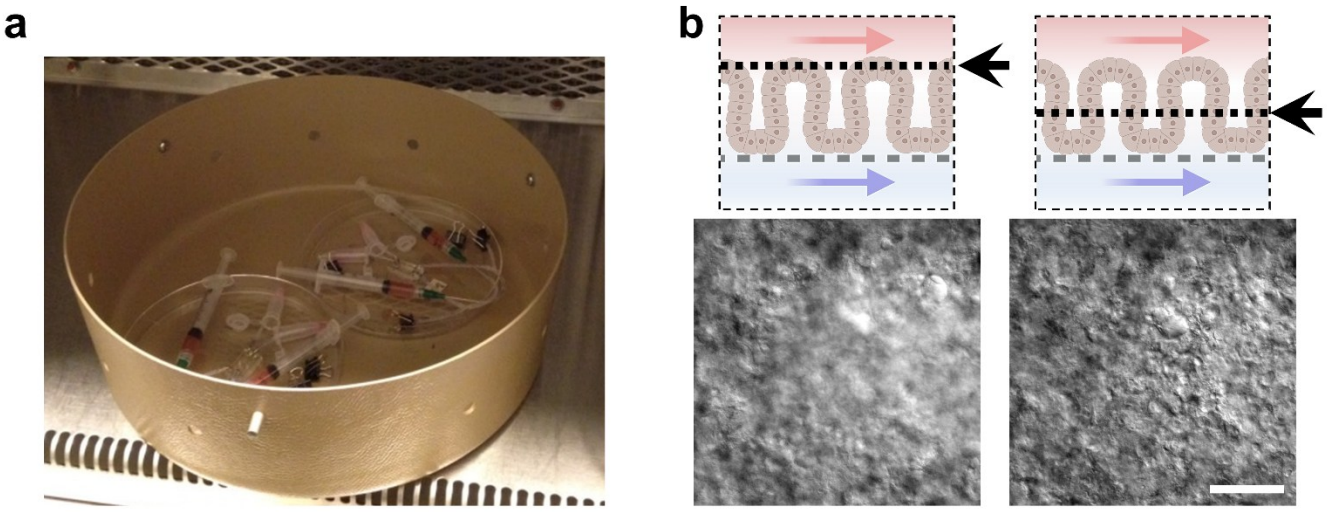

Supplementary Fig. S1. Gamma irradiation setup and post-irradiation morphological assessment. (**a**) Representative gamma irradiation setup showing two gut-on-a-chip devices placed within the round chamber of the Gammacell 40 Exactor. For “Irr. Med.” and “Irr. All” experiments, culture medium in a 50-mL tube was irradiated under identical conditions. For “Irr. Cells” experiments, irradiated syringes were replaced with non-irradiated ones. (**b**) Schematic illustration indicating the focal plane position and corresponding representative DIC micrographs of post-irradiation morphologies. The grey dashed line in the schematic denotes the basement membrane location. Pink and blue arrows indicate the direction of culture medium flow in the upper and lower microchannels, respectively. Black arrows and dashed lines mark the optical plane at which DIC images were acquired. Bar, 100 μm.

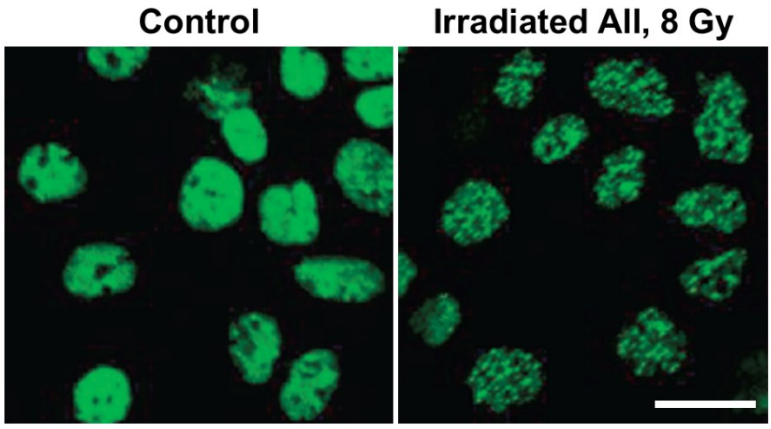

Supplementary Fig. S2. Formation of double-strand DNA damage foci in a 2D Caco-2 monolayer following irradiation under static culture conditions. A Caco-2 monolayer pre-cultured on an ECM-coated glass-bottom plate under static conditions was exposed to 8 Gy irradiation, followed by incubation at 37 ºC in a CO_2 incubator for 5 h with irradiated medium. Cells were then immunofluorescently labeled with anti-53BP1 antibodies. The presence of multiple foci indicates sites of double-strand DNA breaks. Bar, 20 μm.

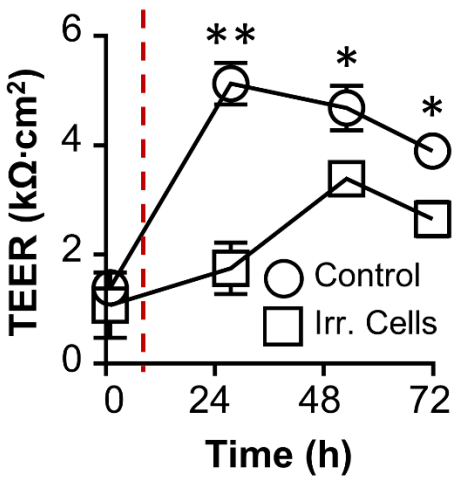

Supplementary Fig. S3. Barrier function assessment via transepithelial electrical resistance measurement. Assessment of epithelial barrier function over time using TEER measurements following exposure to irradiated medium for 90 h (*n*=4). The red dashed line indicates the time point of irradiation. *p<0.05; **p<0.001.

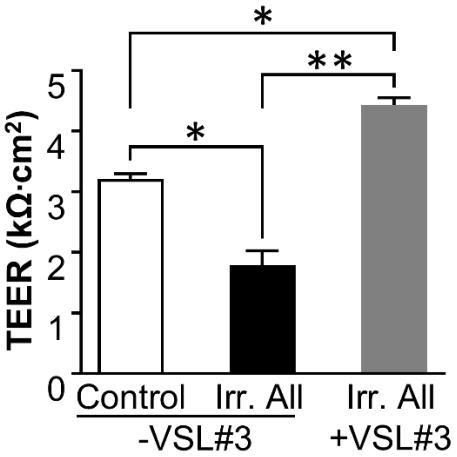

Supplementary Fig. S4. Probiotic VSL#3 preserves epithelial barrier integrity following irradiation. Assessment of epithelial barrier function in control (*n*=2), Irr. All -VSL#3 (*n*=2), and Irr. All +VSL#3 (*n*=4) conditions at 48 h after irradiation. *$p<0.01$; **$p<0.001$.

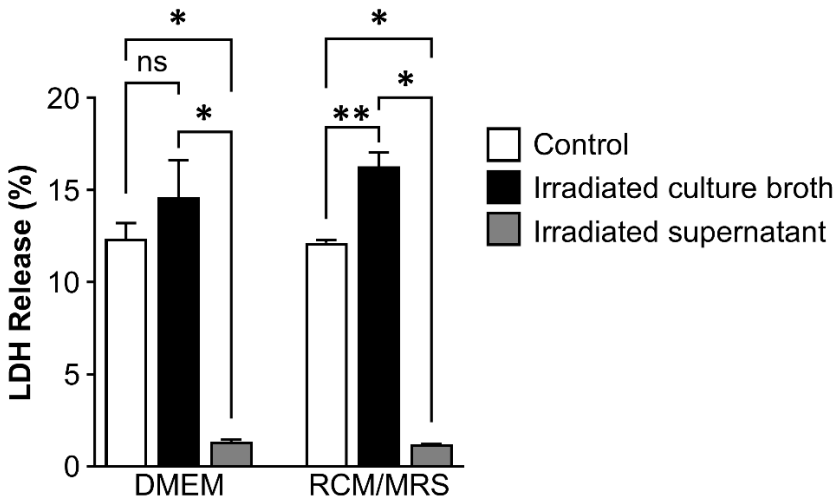

Supplementary Fig. S5. Background LDH signals detected in probiotic VSL#3 cultures. Culture broths of VSL#3 cells grown in either DMEM or RCM/MRS bacterial medium were assessed to determine background LDH activity. “Control” represents the culture broth of VSL#3 cells (final density, 1×10^7 CFU/mL) grown in each medium. “Irradiated culture broth” denotes the samples of the whole VSL#3 culture broth irradiated at 8 Gy in each medium. “Irradiated supernatant” refers to the irradiated samples (8 Gy) prepared from culture supernatants obtained by centrifugation (10,000× *g*, 5 min) of each culture broth. Data are shown as mean ± SEM (*n*=3). *p<0.0001; **p<0.05.

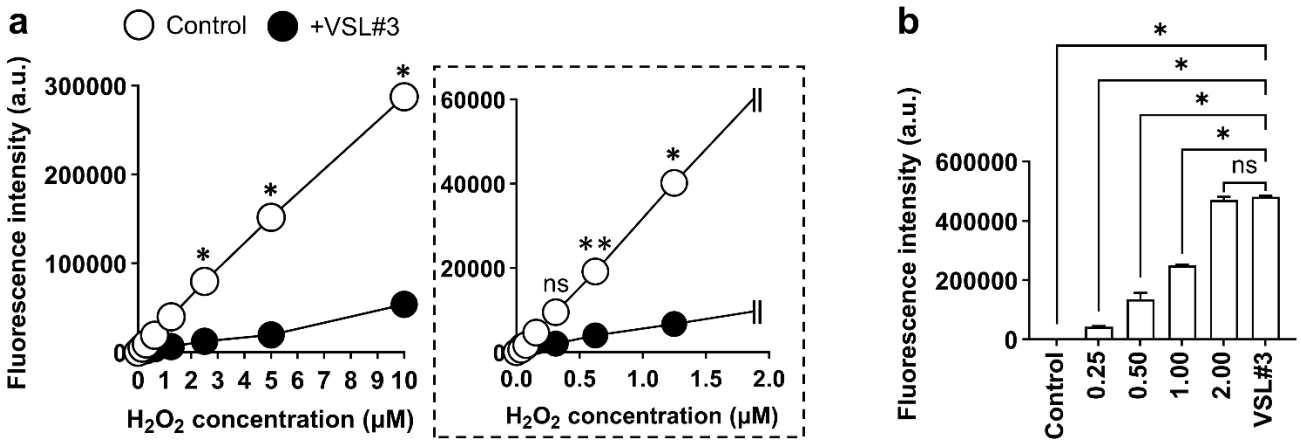

Supplementary Fig. S6. Probiotic VSL#3 exhibits H_2O_2 scavenging and peroxidase activities. (**a**) Fluorescence quantification of reactions between 0.2 U/mL horseradish peroxidase (HRP) and 100 μM Amplex Red reagent with varying H_2O_2 concentrations in the absence or presence of VSL#3 cells (*n*=2). The dashed inset highlights the lower concentration range; no statistically significant differences were observed for concentrations <0.5 μM. Fluorescence intensity is directly proportional to H_2O_2 concentration. **p*<0.001; ***p*<0.05; ns, not significant. (**b**) Fluorescence quantification of reactions between 2 mM H_2O_2 and 100 μM Amplex Red reacting with either varying HRP concentrations (0-2.00 mU/mL) or VSL#3 (*n*=2). Fluorescence intensity is directly proportional to peroxidase concentration. **p*<0.001; ns, not significant. The Control reaction contains neither HRP nor bacteria.

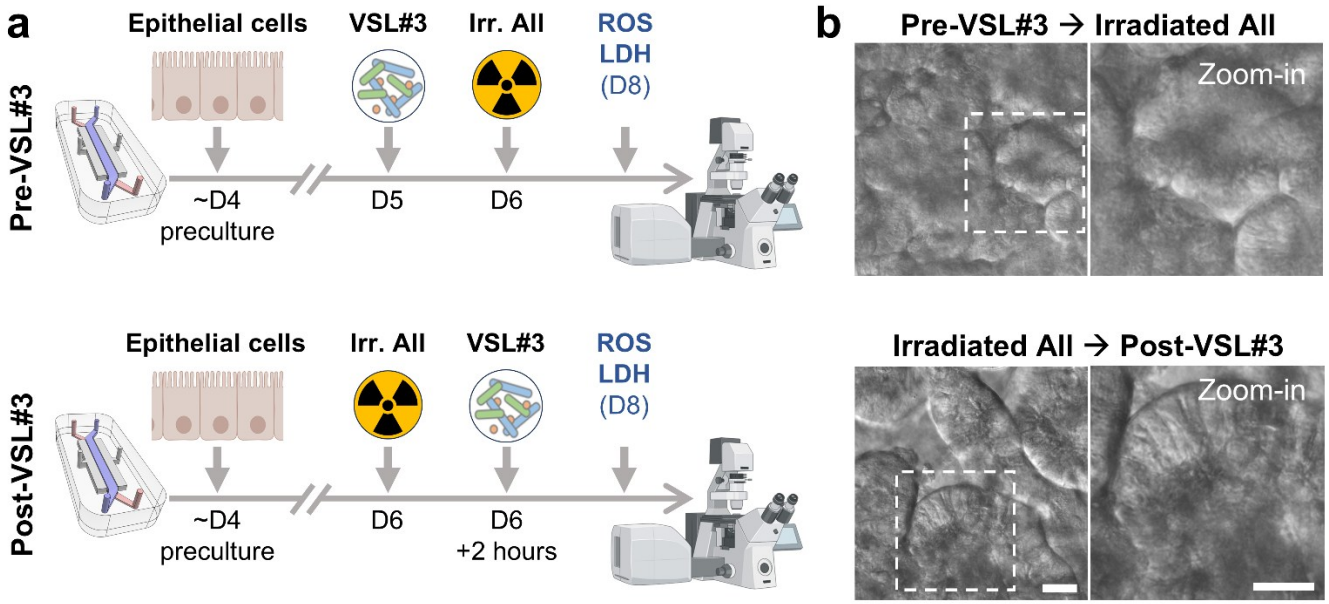

Supplementary Fig. S7. Probiotic VSL#3 attenuates radiation-induced morphological disruption in a gut-on-a-chip. (**a**) Schematic overview of the experimental workflow. "Post-VSL#3" denotes the timing of probiotic administration, which was following gamma irradiation of both epithelial cells and culture medium. Post-exposure assessments included intracellular ROS quantification via microfluorimetry and cytotoxicity evaluation through LDH assays conducted on culture supernatants. (**b**) DIC images depicting epithelial morphology 48 h post-irradiation and irradiated medium perfusion, with either pre- or post-treatment with VSL#3. Pre-treatment preserved epithelial contours, while post-treatment appeared to further enhance structural recovery. Bars, 25 μm.

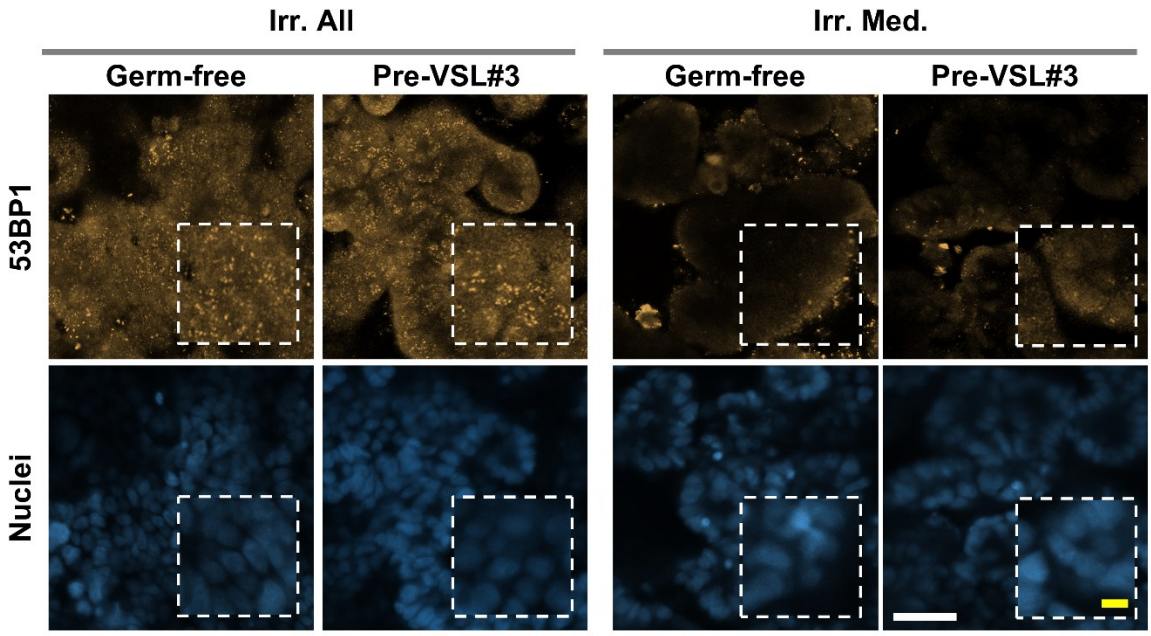

Supplementary Fig. S8. Probiotic VSL#3 does not alter radiation-induced DNA damage response. Representative immunofluorescence micrographs showing independent signals of 53BP1 and Nuclei in 3D Caco-2 cells subjected to either “Irr. All” (direct irradiation followed by exposure to irradiated medium) or “Irr. Med.” (intact Caco-2 cells exposed to irradiated medium), in the presence or absence of VSL#3 cells. The individual fluorescence channels corresponding to the overlaid images in Fig. 5 are shown separately. Yellow bar, 20 μm; White bar, 50 μm.